



RESEARCH MEMORANDUM

for the

Bureau of Aeronautics, Department of the Navy

WIND-TUNNEL INVESTIGATION AT LOW SPEED OF PITCHING

DERIVATIVES OF A 0.085-SCALE MODEL OF THE

CHANCE VUGHT XF8U-1 AIRPLANE

TED NO. NACA DE 392

By Byron M. Jaquet and James L. Williams

Langley Aeronautical Laboratory
Langley Field, Va.

CLASSIFIED DOCUMENT

This material contains information affecting the National Defense of the United States within the meaning of the espionage laws, Title 18, U.S.C., Secs. 793 and 794, the transmission or revelation of which in any manner to an unauthorized person is prohibited by law.

NATIONAL ADVISORY COMMITTEE
FOR AERONAUTICS
WASHINGTON

UNCLASSIFIED



NATIONAL ADVISORY COMMITTEE FOR AERONAUTICS

RESEARCH MEMORANDUM

for the

Bureau of Aeronautics, Department of the Navy

WIND-TUNNEL INVESTIGATION AT LOW SPEED OF PITCHING

DERIVATIVES OF A 0.085-SCALE MODEL OF THE

CHANCE VUGHT XF8U-1 AIRPLANE

TED NO. NACA DE 392

By Byron M. Jaquet and James L. Williams

NASA A. GEN # 70
7-20-66
8-30-66
Lent

SUMMARY

At the request of the Bureau of Aeronautics, Department of the Navy, an investigation was made in the Langley stability tunnel in order to determine the pitching derivatives at low speed of a 0.085-scale model of the Chance Vought XF8U-1 airplane. The complete model was tested through an angle-of-attack range of -6° to 36° for three clean configurations and one landing configuration and with the horizontal and vertical tails removed for one clean configuration and the landing configuration. Tests were also made with the complete model in order to determine the effects of external stores and horizontal-tail incidence on the derivatives.

In order to expedite publication no analysis of the data has been made.

INTRODUCTION

In the development of an airplane an accurate knowledge of the stability derivatives and mass characteristics is necessary in order to insure accurate estimates of the dynamic stability. Although experimental data are available concerning the effects of airplane geometry on the pitching derivatives of various model configurations (see ref. 1, for example), these data are of a general nature and, for a specific airplane, wind-tunnel tests of a scale model are necessary in order to obtain accurate derivatives.

UNCLASSIFIED

As an aid in the development program of the Chance Vought XF8U-1 airplane, the present investigation, made in the Langley stability tunnel, was requested by the Bureau of Aeronautics, Department of the Navy. The purpose of this investigation was to determine the pitching derivatives, through an angle-of-attack range of -6° to 36° , for three clean configurations and one landing configuration of a 0.085-scale complete model of the Chance Vought XF8U-1 airplane. For one clean configuration and the landing configuration, the model was tested with the horizontal and vertical tails removed. In addition, tests were made in order to determine the effect of external stores and horizontal-tail incidence on the complete-model derivatives.

The static longitudinal and static lateral stability characteristics and the yawing derivatives of the same model are presented in reference 2.

SYMBOLS AND COEFFICIENTS

The data presented herein are in the form of standard NACA symbols and coefficients of forces and moments and are referred to the stability system of axes shown in figure 1. The coefficients are based on the dimensions of the wing plan form neglecting the chord-extension. The center of gravity was located at 0.287 of the mean aerodynamic chord. The coefficients and symbols used herein are defined as follows:

L	lift, lb
D	drag, lb
M	pitching moment, ft-lb
A	aspect ratio, b^2/S
b	span, ft
S	area, sq ft
c	local chord parallel to plane of symmetry, ft
\bar{c}	mean aerodynamic chord $\frac{2}{S} \int_0^{b/2} c^2 dy$, ft
y	spanwise distance measured from and perpendicular to plane of symmetry, ft

l	tail length, distance parallel to fuselage reference line from center of gravity to $\bar{c}/4$ of tail, ft
z	tail height, vertical distance from center of gravity to $\bar{c}/4$ of tail measured perpendicular to fuselage reference line, ft
q_0	dynamic pressure, $\frac{\rho V^2}{2}$, lb/sq ft
ρ	mass density of air, slugs/cu ft
V	airspeed, ft/sec
V'	volume, cu ft
α	angle of attack of fuselage reference line, deg
i_w	angle of incidence of wing with respect to fuselage reference line, deg
i_H	angle of incidence of horizontal tail with respect to fuselage reference line, deg
δ_f	symmetrical deflection of trailing-edge control, measured perpendicular to hinge line, deg
$\delta_{I.L.E.}$	deflection of inboard wing leading edge, deg (see fig. 2)
$\delta_{O.L.E.}$	deflection of outboard wing leading edge, deg (see fig. 2)
θ	angle of pitch, radians
γ	angle of climb, radians
$\frac{q\bar{c}}{2V}$	pitching angular velocity parameter, radians
$q = \frac{d\theta}{dt}$	pitching velocity, radians/sec
C_L	lift coefficient, $L/q_0 S_w$
C_D	drag coefficient, $D/q_0 S_w$
C_m	pitching-moment coefficient, $M/q_0 S_w \bar{c}$

$$C_{Lq} = \frac{\partial C_L}{\partial \frac{q\bar{c}}{2V}}$$

$$C_{Dq} = \frac{\partial C_D}{\partial \frac{q\bar{c}}{2V}}$$

$$C_{mq} = \frac{\partial C_m}{\partial \frac{q\bar{c}}{2V}}$$

Subscripts:

w	wing
V	vertical tail
H	horizontal tail
F	fuselage

APPARATUS, MODEL, AND TESTS

The 6- by 6-foot curved-flow test section (ref. 3) of the Langley stability tunnel was used for the present investigation. In this test section curved flight is simulated by curving the airstream about a model that is rigidly mounted to a support strut. The support strut in turn is rigidly mounted to a six-component balance system.

The model used in the present investigation (previously used for the investigation of ref. 2) was a 0.085-scale model of the Chance Vought XF8U-1 airplane and was supplied to the NACA by Chance Vought Aircraft. The general arrangement of the model is shown in figure 2 and photographs of the model are presented as figure 3. Additional details concerning the model are given in table I. The chordwise gaps at the inboard edge of the deflectable leading edge, at the inboard edge of the deflectable chord-extension, and along the trailing-edge control were unsealed for the tests as were the spanwise gaps along the trailing-edge control hinge line. For the present investigation, the trailing-edge control was used as a flap although it is both a flap and an aileron. For all tests, the spanwise gaps along the hinge line of the deflectable leading edge were

sealed on the upper and lower surfaces with plastic tape. The various model configurations tested are indicated in the following table:

i_w , deg	i_H , deg	$\delta_{I.L.E.}$, deg	$\delta_{O.L.E.}$, deg	δ_f , deg	Components	Stores
Clean Configuration						
-1	0	0	0	0	WVH	Off
-1	0	0	6.8	0	WVH	Off
-1	0	6.8	6.8	0	WVH	Off
-1	---	0	0	0	WF	Off
-1	-10	0	0	0	WVH	Off
-1	0	0	0	0	WVH	Inboard and outboard on
-1	0	0	0	0	WVH	Outboard on
Landing Configuration						
7	0	20	30	20	WVH	Off
7	---	20	30	20	WF	Off
7	-10	20	30	20	WVH	Off
7	0	20	30	20	WVH	Inboard and outboard on
7	0	20	30	20	WVH	Outboard on

where

WF wing + fuselage

WVH wing + fuselage + vertical tail + horizontal tail

The tests consisted of the measurement of lift, drag, and pitching moment through an angle-of-attack range of -6° to 36° . The test Mach number was 0.13 and the test Reynolds number was 0.93×10^6 based on a dynamic pressure of 24.9 lb/sq ft and the mean aerodynamic chord of the wing plan form without the chord-extension ($\bar{c}_w = 1.001$ ft). Each of the model configurations was tested at values of $\frac{qc}{2V}$ of 0, 0.0104, 0.0220, and 0.0290.

CORRECTIONS

Approximate jet boundary corrections derived for unswept wings (ref. 4) were applied to the angle of attack and drag coefficient.

Blockage corrections were determined by the methods of reference 5 and were applied to the dynamic pressure and the drag coefficient. Horizontal-tail-on pitching-moment coefficients were corrected for the effects of the jet boundaries by the methods of reference 6.

In curved flow, a pressure gradient across the tunnel exists and this condition necessitates the following corrections:

$$\Delta C_{Lq} = \frac{4}{\bar{c}_w S_w} \left[V_w' + V_V' + V_H' + V_F' (1 + 0.06 \cos^2 \alpha + 1.92 \sin^2 \alpha) \right]$$

$$C_{Lq} = (C_{Lq})_T - \Delta C_{Lq}$$

$$\Delta C_{mq} = \Delta C_{Lq} \frac{r'}{\bar{c}_w} \cos(180^\circ - \alpha)$$

$$C_{mq} = (C_{mq})_T + \Delta C_{mq}$$

where the subscript T refers to the uncorrected value of a given derivative. The correction to \bar{C}_{mq} arises from the fact that for this model the center of volume and center of gravity do not coincide. The center of volume is 2 inches forward of the center of gravity; thus, $r' = \frac{1}{6}$ ft in the equation for ΔC_{mq} . Corrections to account for the effects of the support strut on the derivatives have not been applied.


RESULTS


Presentation of Results

The variation of C_{Lq} , C_{Dq} , and C_{mq} with α is presented in figure 4 for various clean model configurations and in figure 5 for various landing model configurations.

The data are tabulated in table II because some of the data points are difficult to distinguish in figure 4. In order to expedite publication of the data presented herein no analysis has been made.

Langley Aeronautical Laboratory,
National Advisory Committee for Aeronautics,
Langley Field, Va., January 20, 1954.


Byron M. Jaquet
Aeronautical Engineer


James L. Williams
Aeronautical Research Scientist

Approved:



Thomas A. Harris
Chief of Stability Research Division

pwg

REFERENCES

1. Lichtenstein, Jacob H.: Experimental Determination of the Effect of Horizontal-Tail Size, Tail Length, and Vertical Location on Low-Speed Static Longitudinal Stability and Damping in Pitch of a Model Having 45° Sweptback Wing and Tail Surfaces. NACA Rep. 1096, 1952. (Supersedes NACA TN's 2381 and 2382.)
2. Jaquet, Byron M., and Williams, James L.: Wind-Tunnel Investigation at Low Speed of Static and Yawing Characteristics of a 0.085-Scale Model of the Chance Vought XF8U-1 Airplane - TED NO. NACA DE 392. NACA SL54A26, Bur. Aero., 1954.
3. Bird, John D., Jaquet, Byron M., and Cowan, John W.: Effect of Fuselage and Tail Surfaces on Low-Speed Yawing Characteristics of a Swept Wing Model as Determined in Curved-Flow Test Section of the Langley Stability Tunnel. NACA TN 2483, 1951. (Supersedes NACA RM L8G13.)
4. Silverstein, Abe, and White, James A.: Wind-Tunnel Interference With Particular Reference to Off-Center Positions of the Wing and to the Downwash at the Tail. NACA Rep. 547, 1936.
5. Herriot, John G.: Blockage Corrections for Three-Dimensional-Flow Closed-Throat Wind Tunnels, With Consideration of the Effect of Compressibility. NACA Rep. 995, 1950. (Supersedes NACA RM A7B28.)
6. Gillis, Clarence L., Polhamus, Edward C., and Gray, Joseph L., Jr.: Charts for Determining Jet-Boundary Corrections for Complete Models in 7- by 10-Foot Closed Rectangular Wind Tunnels. NACA WR L-123, 1945. (Formerly NACA ARR L5G31.)

TABLE I.- DETAILS OF 0.085-SCALE MODEL OF
CHANCE-VOUGHT XF8U-1 AIRPLANE

Wing:

Airfoil section at root	NACA 65A006
Airfoil section at tip	NACA 65A005
Area, S_w , sq ft	2.715
Span, b_w , ft	3.043
Mean aerodynamic chord, (without chord extension), \bar{c}_w ft	1.001
Root chord (on fuselage reference line), ft	1.430
Tip chord (without chord-extension), ft	0.352
Tip chord (with chord-extension), ft	0.394
Sweep of $c/4$, deg	42
Dihedral, deg	-5
Aspect ratio, A_w	3.4
Taper ratio (without chord-extension)	0.25

Horizontal tail:

Airfoil section at root	NACA 65A006
Airfoil section at tip	NACA 65A004
Area, S_H , sq ft	0.766
Span, b_H , ft	1.638
Root chord (on fuselage reference line), ft	0.814
Tip chord, ft	0.122
Sweep of $c/4$, deg	45
l_H , ft	1.56
Dihedral, deg	5.42
Area ratio, S_H/S_w	0.282
Aspect ratio	3.5
Taper ratio	0.15

Vertical tail:

Airfoil section at root	NACA 65A006
Airfoil section at tip	NACA 65A004
Area, S_v , sq ft	0.722
Span (measured from fuselage reference line) b_v , ft	1.028
Root chord (on fuselage reference line), ft	1.115
Tip chord, ft	0.291
Sweep of $c/4$, deg	45
l_v , ft	1.230
z_v , ft	0.412
Area ratio, S_v/S_w	0.266
Aspect ratio	1.47
Taper ratio	0.26

TABLE II.- TABULATION OF DATA

α , deg	C_{Lq}	C_{Dq}	C_{mq}	α , deg	C_{Lq}	C_{Dq}	C_{mq}
Figure 4; symbol \bigcirc				Figure 4; symbol \diamond			
-6.30	4.508	-0.665	-4.614	-6.29	3.636	-0.621	-4.535
-4.21	4.159	-.502	-4.468	-4.22	3.712	-.537	-4.321
-2.12	3.703	-.379	-4.302	-2.13	3.516	-.409	-4.257
-.04	3.668	-.291	-4.328	-.04	3.511	-.325	-4.193
2.03	3.836	-.054	-4.504	2.04	3.289	-.207	-4.430
4.12	3.755	.103	-4.671	4.12	3.385	-.049	-4.814
6.21	3.425	.187	-4.634	6.20	3.444	.113	-5.028
8.30	3.182	.217	-4.762	8.28	3.365	.236	-4.990
10.39	2.741	.222	-4.326	10.38	3.126	.384	-4.613
12.48	2.714	.468	-4.300	12.47	2.970	.438	-4.270
14.57	2.182	.463	-4.255	14.54	2.685	.365	-4.319
16.64	1.985	.148	-4.337	16.65	2.482	.478	-4.293
18.72	1.808	.640	-4.266	18.73	2.773	.709	-4.625
20.76	.426	.084	-3.850	20.79	2.315	.761	-4.545
22.78	-.495	-.044	-4.506	22.83	-.964	.222	-3.908
24.81	.244	.256	-4.387	24.87	-.152	.615	-5.192
26.85	-1.050	-.261	-4.101	26.88	-2.158	-.291	-4.681
28.87	-1.551	-.414	-3.592	28.90	-3.236	-.729	-3.897
30.90	-3.022	-.956	-1.640	30.92	-3.613	-.739	-1.675
32.92	-3.966	-1.517	-.323	32.96	-5.370	-2.207	.327
34.93	-2.802	-1.207	-2.103	34.95	-3.467	-1.325	-1.734
36.94	-2.613	-.921	-2.948	36.95	-3.002	-1.039	-3.012
Figure 4; symbol \square				Figure 4; symbol \triangle			
-6.29	4.223	-0.591	-4.437	-6.28	2.131	-0.388	-0.998
-4.21	3.873	-.537	-4.257	-4.19	1.597	-.266	-1.010
-2.12	3.516	-.374	-4.262	-2.11	1.258	-.207	-1.018
-.04	3.491	-.291	-4.154	-.04	1.235	-.113	-1.012
2.03	3.614	-.128	-4.321	2.04	.995	-.069	-1.038
4.12	3.242	-.015	-4.528	4.12	1.066	.044	-.975
6.20	3.301	.079	-4.663	6.20	.776	.049	-1.080
8.29	3.464	.236	-4.838	8.28	1.164	.138	-1.082
10.38	3.110	.333	-4.552	10.37	.765	.098	-1.118
12.48	2.897	.401	-4.514	12.46	.385	.064	-1.194
14.56	2.827	.443	-4.486	14.54	.313	-.010	-1.267
16.63	2.164	.671	-4.324	16.60	.194	.251	-1.301
18.72	1.990	.512	-4.630	18.66	-.465	-.049	-1.318
20.77	1.842	.542	-4.486	20.68	-2.023	-.539	-1.060
22.83	-.180	.101	-3.948	22.69	-1.941	-.606	-1.282
24.84	-1.318	-.034	-4.858	24.68	-1.952	-.679	-1.395
26.86	-1.057	-.059	-4.495	26.72	-2.384	-.990	-1.523
28.89	-1.610	-.374	-4.168	28.74	-2.928	-1.122	-1.684
30.91	-2.312	-.498	-2.428	30.75	-2.710	-1.023	-1.732
32.95	-5.030	-2.158	-.018	32.79	-3.454	-1.759	-1.834
34.94	-3.541	-1.488	-1.783	34.80	-3.284	-1.537	-1.822
36.95	-3.283	-1.483	-2.702	36.80	-3.420	-1.700	-1.829

TABLE II.- TABULATION OF DATA - Continued

α , deg	C_{Lq}	C_{Dq}	C_{mq}	α , deg	C_{Lq}	C_{Dq}	C_{mq}
Figure 4; symbol \triangle				Figure 4; symbol \square			
-6.32	4.482	-0.876	-4.097	-6.28	4.154	-0.557	-4.338
-4.24	4.453	-.808	-4.011	-4.21	4.060	-.424	-4.281
-.08	3.858	-.492	-4.068	-.04	3.732	-.256	-4.193
4.08	3.750	-.128	-4.405	4.11	3.390	.020	-4.494
8.26	2.679	-.212	-4.330	8.31	3.217	.192	-4.646
12.44	2.860	-.227	-4.270	12.49	2.467	.246	-4.443
16.60	2.398	.182	-4.943	16.65	2.379	.054	-4.337
20.70	.870	-.139	-5.040	18.73	2.488	.768	-4.507
24.75	-.249	-.315	-5.219	20.78	1.088	.310	-3.994
28.83	-1.191	-.576	-4.868	22.79	-.317	.064	-4.610
32.89	-1.695	-.675	-4.436	24.81	-1.352	-.340	-4.154
36.92	-2.899	-.635	-2.514	28.88	-1.433	-.197	-3.661
				32.93	-4.636	-1.640	-.023
				36.95	-3.386	-1.379	-2.421
Figure 4; symbol ∇				Figure 5; symbol \circ			
-6.28	3.755	-0.557	-4.200	-5.90	2.208	-0.419	-4.023
-4.21	3.981	-.502	-4.016	-3.81	2.134	-.443	-4.119
-2.12	3.767	-.409	-4.051	-1.73	2.057	-.335	-4.400
-.04	3.511	-.261	-3.977	.35	2.112	-.246	-4.578
2.04	3.368	-.172	-4.321	2.42	2.368	-.123	-4.661
4.12	3.469	-.005	-4.454	4.50	2.962	.044	-4.863
6.20	3.380	.079	-4.658	6.56	2.657	.143	-4.885
8.31	2.947	.232	-4.542	8.64	2.548	.158	-4.784
10.39	2.794	.241	-4.061	10.73	2.421	.276	-4.824
12.48	2.856	.424	-4.009	12.79	2.106	.163	-4.539
14.56	2.581	.507	-4.058	14.85	2.246	.453	-4.900
16.64	2.871	.315	-4.367	16.90	2.136	.236	-4.613
18.72	2.557	.803	-4.285	18.91	2.015	.453	-4.394
20.77	1.635	.640	-3.683	20.93	.985	.177	-4.141
22.80	.069	.286	-4.531	22.93	.747	.034	-4.580
24.81	-.397	.202	-4.362	24.93	.485	-.453	-4.809
26.86	-1.301	-.404	-3.974	26.93	.340	-.640	-4.678
28.88	-1.970	-.419	-3.745	28.93	.085	-1.128	-4.055
30.91	-3.184	-.995	-2.069	30.93	-2.554	-1.468	-1.818
32.94	-4.423	-1.877	.071	32.95	-4.598	-2.222	.303
34.97	-5.096	-2.246	.044	34.93	-3.211	-1.665	-2.472
36.94	-2.949	-1.241	-1.908	36.90	-2.815	-1.379	-3.337

TABLE II.- TABULATION OF DATA - Concluded

α , deg	C_{Lq}	C_{Dq}	C_{mq}	α , deg	C_{Lq}	C_{Dq}	C_{mq}
Figure 5; symbol \square				Figure 5; symbol \triangle			
-5.87	0.456	-0.172	-1.154	-5.91	1.957	-0.310	-3.422
-3.79	.282	-.241	-1.009	-3.82	1.656	-.266	-3.632
-1.69	.005	-.236	-.836	.34	1.401	-.148	-3.829
.38	.064	-.271	-.860	4.49	2.213	.059	-3.962
2.45	.241	-.197	-.953	8.65	1.331	.202	-4.252
4.52	.199	-.369	-.950	12.79	.487	.182	-3.743
6.59	.475	-.143	-1.090	16.89	-.552	-.044	-4.894
8.67	.525	-.138	-1.245	20.97	-1.350	-.926	-5.027
10.74	.434	-.059	-1.276	22.97	-1.303	-.956	-4.456
12.79	.695	-.049	-1.052	24.96	-.249	-1.054	-5.515
14.84	.559	-.015	-1.022	28.95	-.457	-2.118	-4.548
16.87	.411	-.177	-.951	32.97	-1.897	-1.768	-3.180
18.83	.208	.394	-.963	36.94	-3.298	-2.217	-1.485
20.84	-.473	-.389	-.996				
22.83	-1.157	-.241	-.864				
24.84	-1.377	-.793	-.774				
26.83	-1.755	-.892	-.828				
28.80	-1.557	-1.325	-1.140				
30.78	-2.875	-1.586	-.802				
32.78	-3.104	-1.793	-.815				
34.79	-3.201	-2.118	-.738				
36.78	-3.336	-2.182	-.868				
Figure 5; symbol \diamond				Figure 5; symbol ∇			
-5.93	2.567	-0.640	-3.787	-5.90	2.292	-0.315	-3.594
-3.84	2.607	-.591	-3.740	-3.81	1.804	-.300	-3.627
.31	2.550	-.350	-4.105	.34	2.190	-.069	-4.144
4.47	2.469	-.192	-4.144	4.48	3.218	.256	-4.523
8.62	1.681	-.495	-4.123	8.64	3.060	.493	-4.444
12.76	1.595	-.281	-3.970	12.78	2.733	.818	-4.428
16.86	1.241	-.133	-4.323	16.91	.945	.384	-5.567
20.89	.379	-.468	-4.107	20.96	-1.014	-.714	-5.299
22.88	1.156	-.335	-4.560	22.97	-1.420	-.916	-4.299
24.87	1.189	-.054	-5.091	24.95	-1.183	-.709	-4.042
28.87	-.738	-1.261	-4.247	28.93	-.446	-.842	-4.247
32.90	-2.321	-1.488	-3.988	32.96	-1.078	-.808	-3.125
36.93	-2.352	-1.670	-3.628	36.93	-1.099	-.275	-1.948

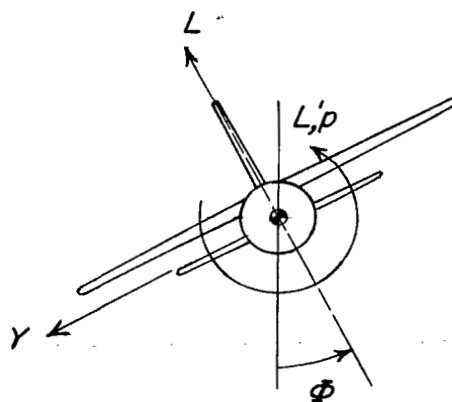
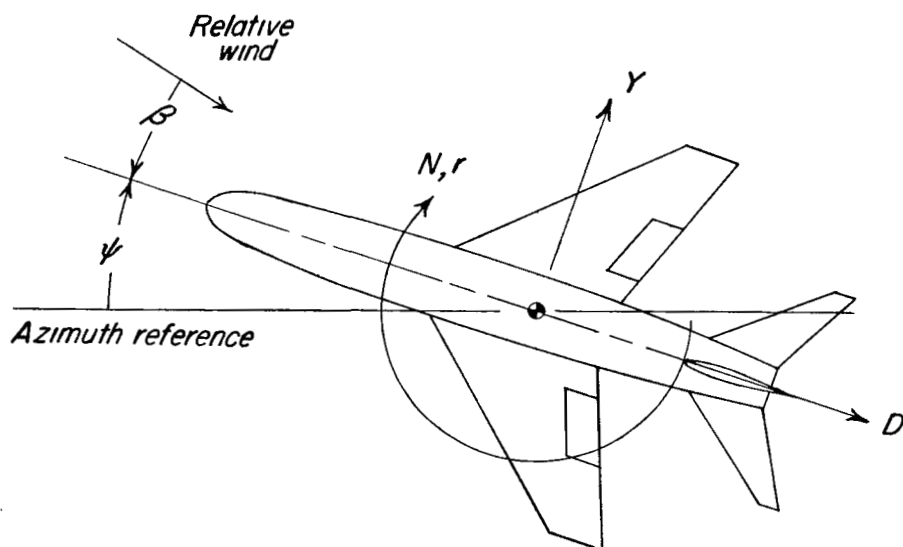
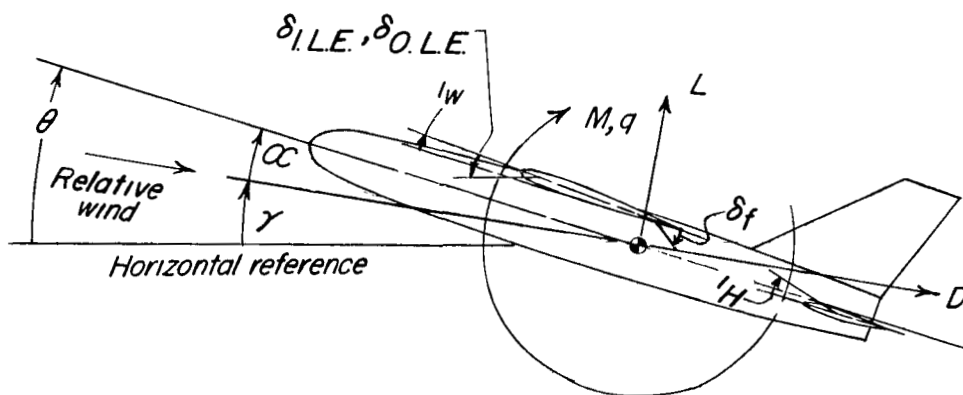


Figure 1.- Stability system of axes. Arrows indicate positive direction of forces, moments, angles, and angular velocities.

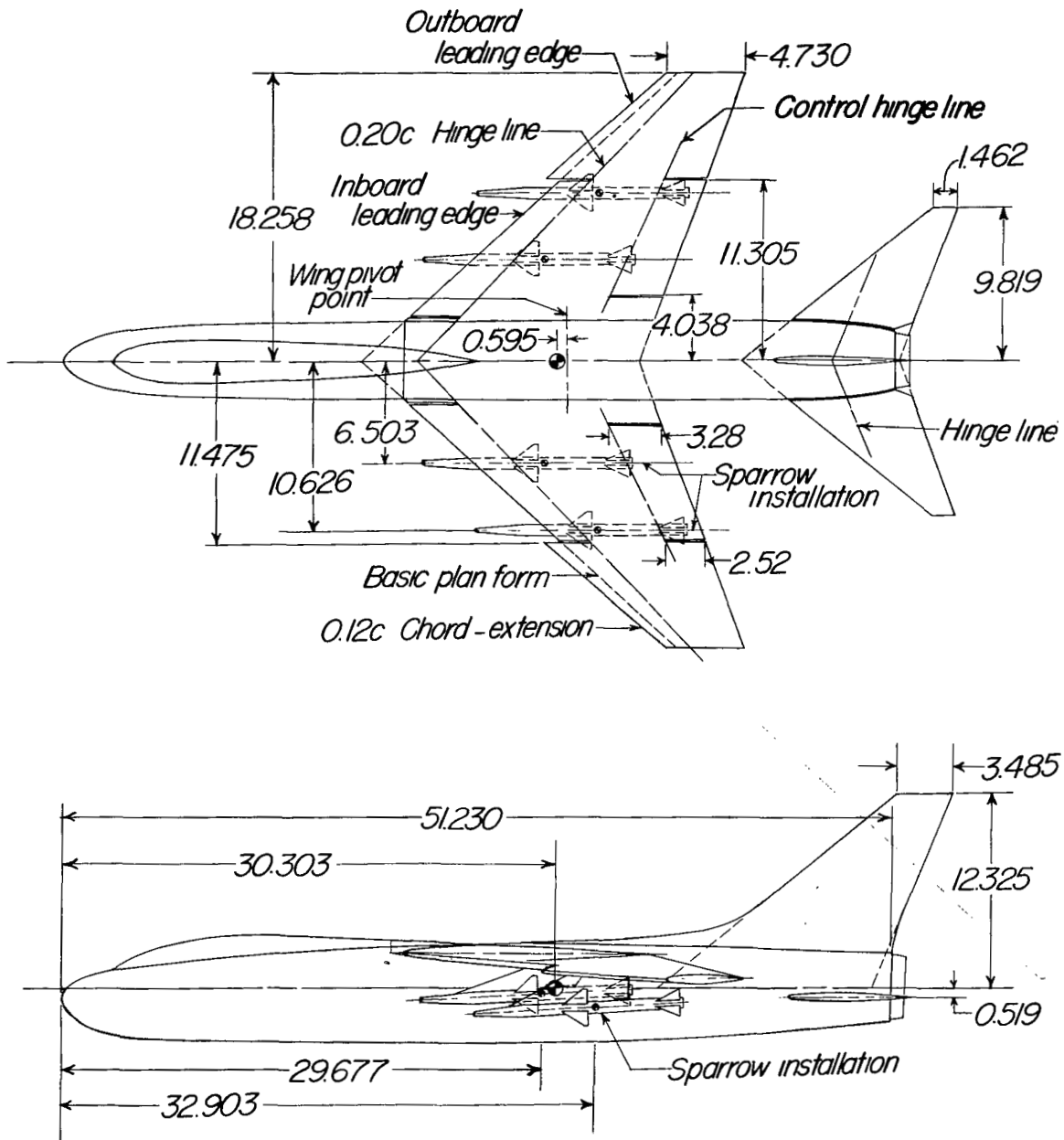
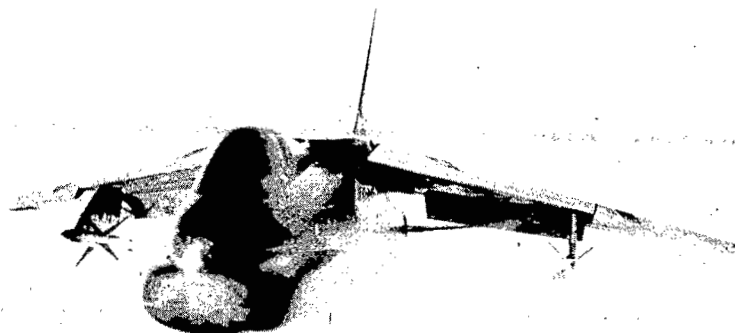


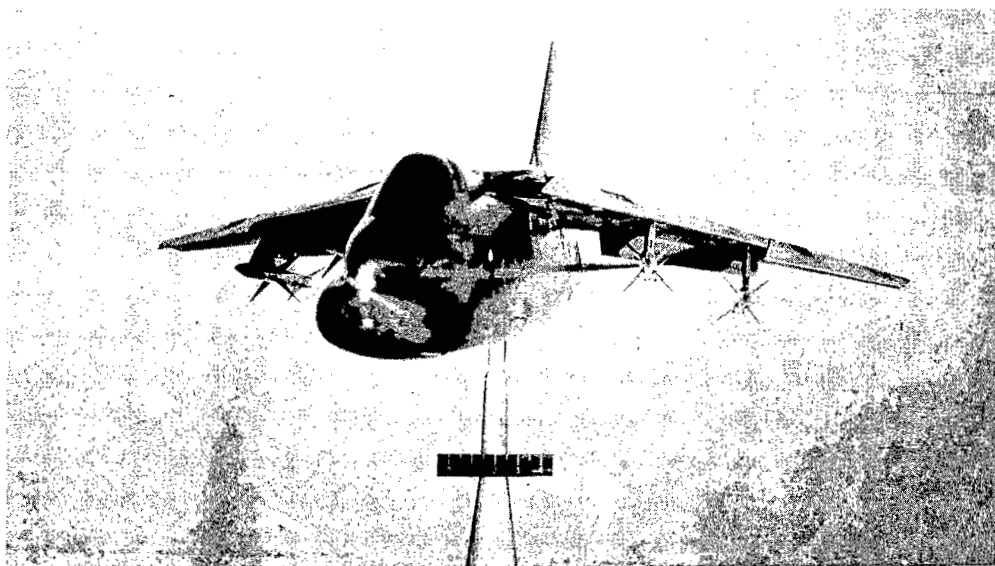
Figure 2.- Details of the 0.085-scale model of the Chance-Vought XF8U-1 airplane. All dimensions are in inches.



111

L-82505

(c) Landing configuration. $i_w = 7^\circ$; $\delta_{I.L.E.} = 20^\circ$; $\delta_{O.L.E.} = 30^\circ$;
 $i_H = 0^\circ$; $\delta_f = 20^\circ$; outboard stores on.



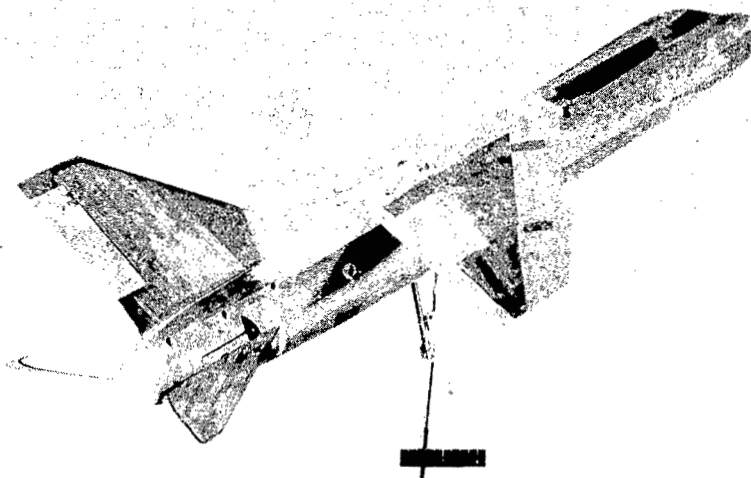
112

L-82506

(d) Landing configuration. $i_w = 7^\circ$; $\delta_{I.L.E.} = 20^\circ$; $\delta_{O.L.E.} = 30^\circ$;
 $i_H = 0^\circ$; $\delta_f = 20^\circ$; inboard and outboard stores on.

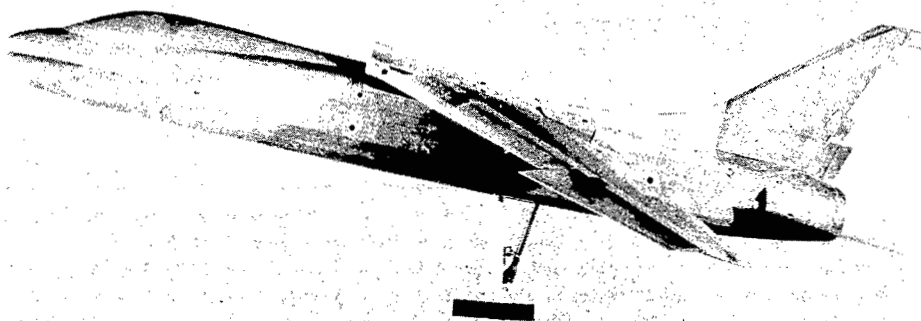
Figure 3.- Concluded.

113



L-82503

(a) Clean configuration. $i_w = -1^\circ$; $\delta_{I.L.E.} = \delta_{O.L.E.} = 0^\circ$; $i_H = 0^\circ$;
 $\delta_f = 0^\circ$.



L-82504

(b) Landing configuration. $i_w = 7^\circ$; $\delta_{I.L.E.} = 20^\circ$; $\delta_{O.L.E.} = 30^\circ$;
 $i_H = 0^\circ$; $\delta_f = 20^\circ$.

Figure 3.- Some model arrangements tested.

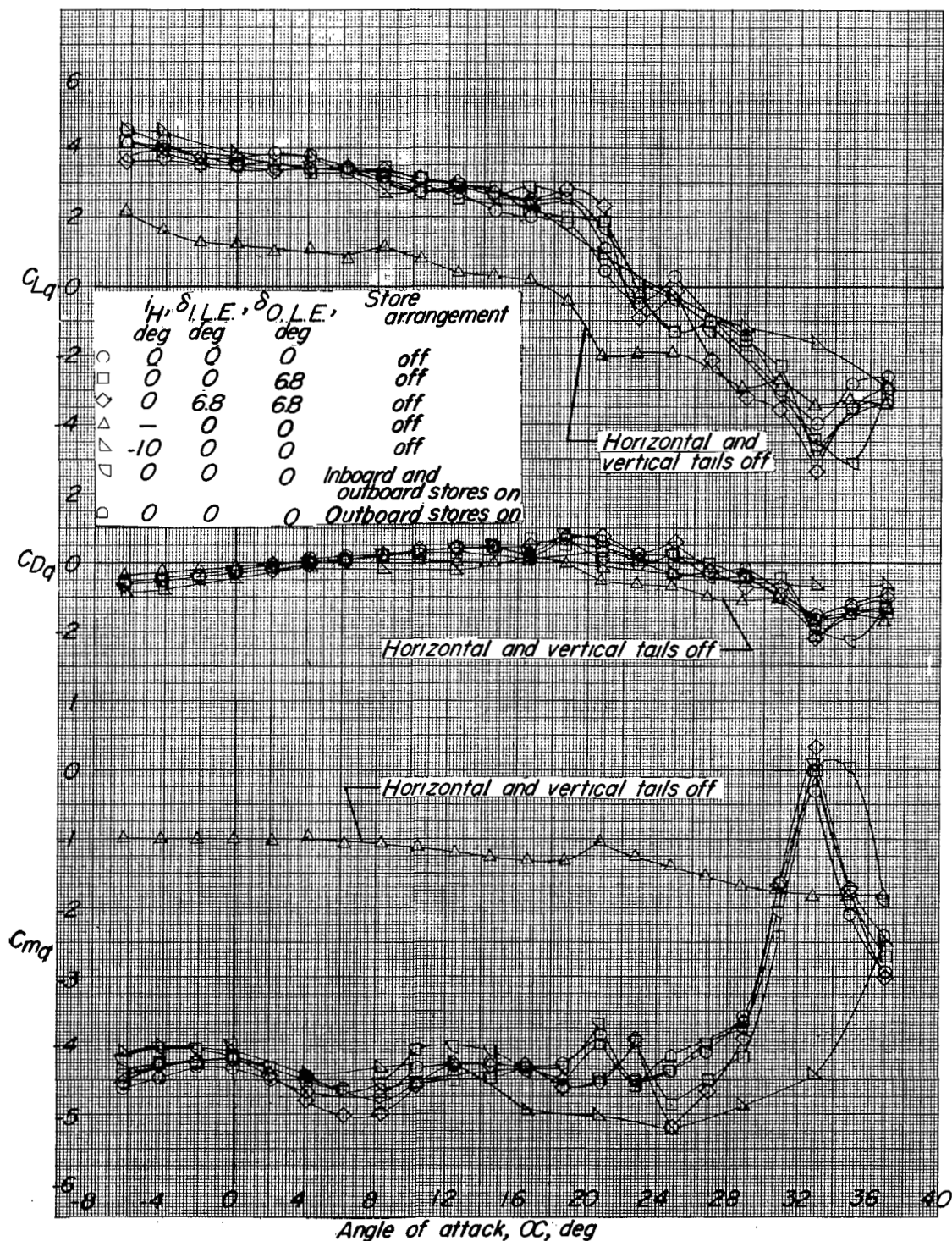


Figure 4.- Variation of C_{Lq} , C_{Dq} , and C_{mq} with α for a 0.085-scale model of the Chance-Vought XF8U-1 airplane. Clean configuration; $\delta_f = 0^\circ$; uncorrected for support strut tares.

UNCLASSIFIED

NACA RM SL54B05a

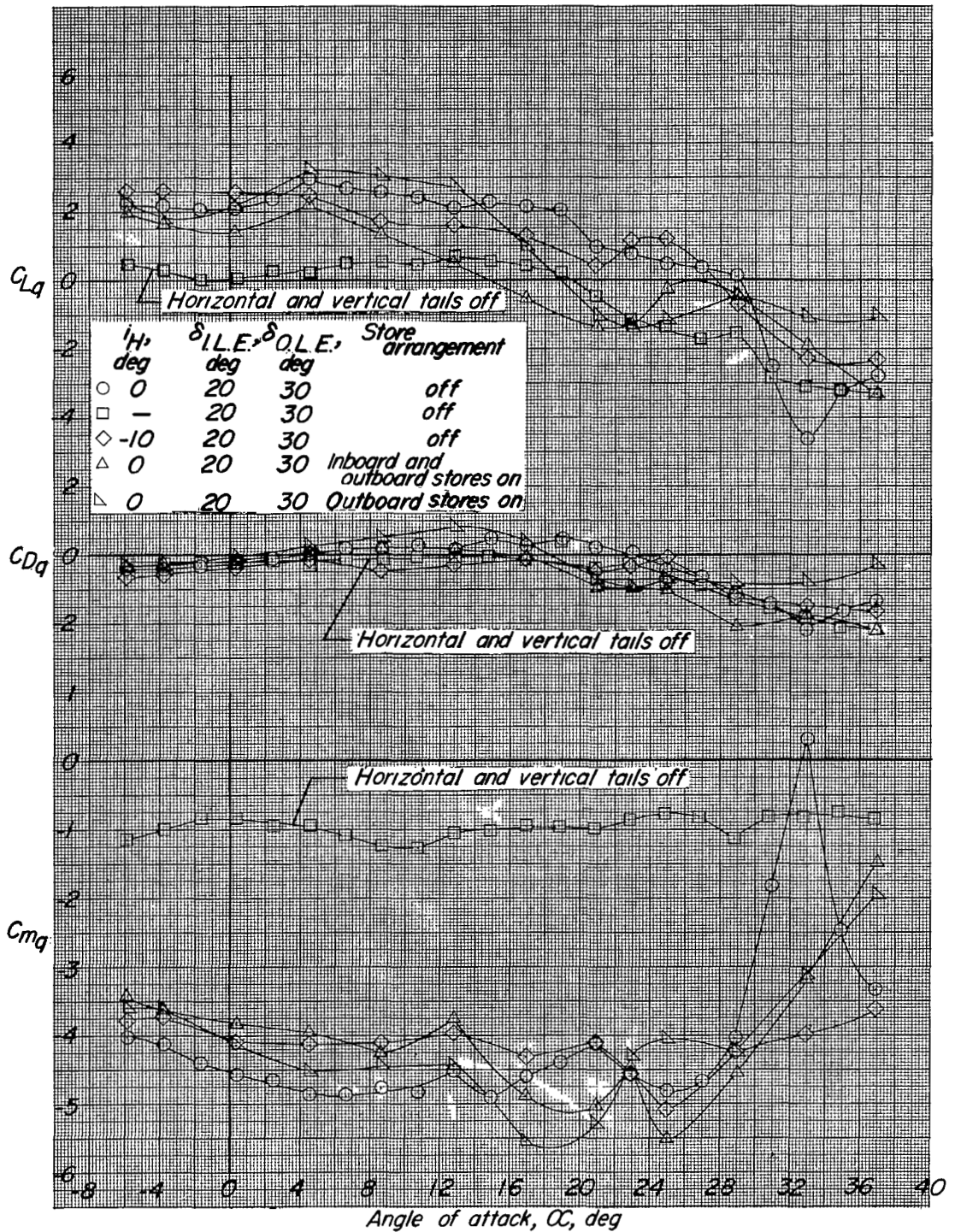


Figure 5.- Variation of C_{Lq} , C_{Dq} , and C_{mq} with α for a 0.085-scale model of the Chance-Vought XF8U-1 airplane. Landing configuration; $\delta_f = 20^\circ$; uncorrected for support strut tares.

NASA Technical Library



3 1176 01438 6768

UNCLASSIFIED